Accepted Manuscript

Synthesis of amide and sulfonamide substituted N-aryl 6-aminoquinoxalines as PFKFB3 inhibitors with improved physicochemical properties

Nicolas Boutard, Arkadiusz Białas, Aleksandra Sabiniarz, Paweł Guzik, Katarzyna Banaszak, Artur Biela, Marcin Bień, Anna Buda, Barbara Bugaj, Ewelina Cieluch, Anna Cierpich, Łukasz Dudek, Hans-Michael Eggenweiler, Joanna Fogt, Monika Gaik, Andrzej Gondela, Krzysztof Jakubiec, Mirek Jurzak, Agata Kitlińska, Piotr Kowalczyk, Maciej Kujawa, Katarzyna Kwiecińska, Marcin Leś, Ralph Lindemann, Monika Maciuszek, Maciej Mikulski, Paulina Niedziejko, Alicja Obara, Henryk Pawlik, Tomasz Rzymski, Magdalena Sieprawska-Lupa, Marta Sowińska, Joanna Szeremeta-Spisak, Agata Stachowicz, Mateusz M. Tomczyk, Katarzyna Wiklik, Łukasz Włoszczak, Sylwia Ziemiańska, Adrian Zarębski, Krzysztof Brzózka, Mateusz Nowak, Charles-Henry Fabritius

PII: S0960-894X(18)30981-8
DOI: https://doi.org/10.1016/j.bmcl.2018.12.034
Reference: BMCL 26203

To appear in: *Bioorganic & Medicinal Chemistry Letters*

Received Date: 7 November 2018
Revised Date: 11 December 2018
Accepted Date: 14 December 2018

Please cite this article as: Boutard, N., Białas, A., Sabiniarz, A., Guzik, P., Banaszak, K., Biela, A., Bień, M., Buda, A., Bugaj, B., Cieluch, E., Cierpich, A., Dudek, L., Eggenweiler, H-M., Fogt, J., Gaik, M., Gondela, A., Jakubiec, K., Jurzak, M., Kitlińska, A., Kowalczyk, P., Kujawa, M., Kwiecińska, K., Leś, M., Lindemann, R., Maciuszek, M., Mikulski, M., Niedziejko, P., Obara, A., Pawlik, H., Rzymski, T., Sieprawska-Lupa, M., Sowińska, M., Szeremeta-Spisak, J., Stachowicz, A., Tomczyk, M.M., Wiklik, K., Włoszczak, L., Ziemiańska, S., Zarębski, A., Brzózka, K., Nowak, M., Fabritius, C-H., Synthesis of amide and sulfonamide substituted N-aryl 6-aminoquinoxalines as PFKFB3 inhibitors with improved physicochemical properties, *Bioorganic & Medicinal Chemistry Letters* (2018), doi: https://doi.org/10.1016/j.bmcl.2018.12.034

Graphical Abstract

To create your abstract, type over the instructions in the template box below.
Fonts or abstract dimensions should not be changed or altered.

Synthesis of amide and sulfonamide substituted *N*-aryl 6-aminoquinoxalines as PFKFB3 inhibitors with improved physicochemical properties

Leave this area blank for abstract info.

Nicolas Boutard, Arkadiusz Białas, Aleksandra Sabiniarz, Paweł Guzik, Katarzyna Banaszak, Artur Biela, Marcin Bień, Anna Buda, Barbara Bugaj, Ewelina Cieluch, Anna Cierpich, Łukasz Dudek, Hans-Michael Eggenweiler, Joanna Fogt, Monika Gaik, Andrzej Gondela, Krzysztof Jakubiec, Mirek Jurzak, Agata Kitlińska, Piotr Kowalczyk, Maciej Kujawa, Katarzyna Kwiecińska, Marcin Leś, Ralph Lindemann, Monika Maciuszek, Maciej Mikulski, Paulina Niedziejko, Alicja Obara, Henryk Pawlik, Tomasz Rzymski, Magdalena Sieprawska-Lupa, Marta Sowińska, Joanna Szeremeta-Spisak, Agata Stachowicz, Mateusz M. Tomczyk, Katarzyna Wiklik, Łukasz Włoszczak, Sylwia Ziemiańska, Adrian Zarębski, Krzysztof Brzózka, Mateusz Nowak, and Charles-Henry Fabritius

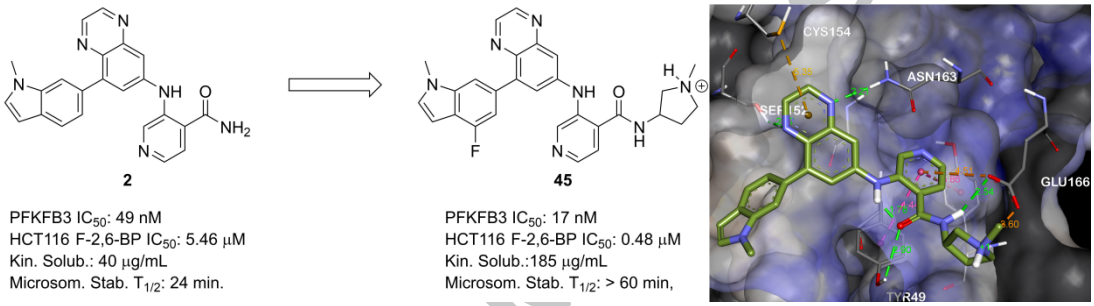

Bioorganic & Medicinal Chemistry Letters
journal homepage: www.elsevier.com/locate/bmcl

Synthesis of amide and sulfonamide substituted *N*-aryl 6-aminoquinoxalines as PFKFB3 inhibitors with improved physicochemical properties

Nicolas Boutard,[a] Arkadiusz Białas,[a] Aleksandra Sabiniarz,[a] Paweł Guzik,[a] Katarzyna Banaszak,[a] Artur Biela,[a] Marcin Bień,[a,c] Anna Buda,[a] Barbara Bugaj,[a] Ewelina Cieluch,[a] Anna Cierpich,[a,d] Łukasz Dudek,[a] Hans-Michael Eggenweiler,[b] Joanna Fogt,[a] Monika Gaik,[a,e] Andrzej Gondela,[a] Krzysztof Jakubiec,[a] Mirek Jurzak,[b] Agata Kitlińska,[a] Piotr Kowalczyk,[a] Maciej Kujawa,[a] Katarzyna Kwiecińska,[a,f] Marcin Leś,[a] Ralph Lindemann,[b] Monika Maciuszek,[a,g¶] Maciej Mikulski,[a] Paulina Niedziejko,[a] Alicja Obara,[a] Henryk Pawlik,[a] Tomasz Rzymski,[a] Magdalena Sieprawska-Lupa,[a] Marta Sowińska,[a] Joanna Szeremeta-Spisak,[a] Agata Stachowicz,[a] Mateusz M. Tomczyk,[a,h] Katarzyna Wiklik,[a] Łukasz Włoszczak,[a,i] Sylwia Ziemiańska,[a] Adrian Zarębski,[a] Krzysztof Brzózka,[a] Mateusz Nowak,[a,*] and Charles-Henry Fabritius[a]

[a] *Selvita S.A., Bobrzyńskiego, 14, 30-338 Kraków, Poland*
[b] *Merck Biopharma, Merck KGaA, Frankfurter Straße 250, 64293 Darmstadt, Germany*

ARTICLE INFO

Keywords:
PFKFB3
N-aryl 6-aminoquinoxalines
Structure-activity relationship
Cancer metabolism
Glycolysis

ABSTRACT

In oncology, the "Warburg effect" describes the elevated production of energy by glycolysis in cancer cells. The ubiquitous and hypoxia-induced 6-phosphofructo-2-kinase/fructose-2,6-biphosphatase 3 (PFKFB3) plays a noteworthy role in the regulation of glycolysis by producing fructose-2,6-biphosphate (F-2,6-BP), a potent activator of the glycolysis rate-limiting phosphofructokinase PFK-1. Series of amides and sulfonamides derivatives based on a *N*-aryl 6-aminoquinoxaline scaffold were synthesized and tested for their inhibition of PFKFB3 *in vitro* in a biochemical assay as well as in HCT116 cells. The carboxamide series displayed satisfactory kinetic solubility and metabolic stability, and within this class, potent lead compounds with nanomolar activity have been identified with a suitable profile for further *in vivo* evaluation.

* Corresponding author. E-mail: mateusz.nowak@selvita.com.
[c] Present address: Almac Group, 20 Seagoe Industrial Estate, Craigavon BT63 5QD, United Kingdom.
[d] Present address: Grupa Azoty S.A., Kwiatkowskiego 8, 33-100 Tarnów, Poland.
[e] Present address: Max Planck Research Group at the Malopolska Centre of Biotechnology, Jagiellonian University, Krakow, Poland
[f] Present address: Captor Therapeutics, Duńska 11, 54-427 Wrocław, Poland.
[g] Present address: LifeArc, Accelerator Building, Open Innovation Campus, Stevenage, SG1 2FX, United Kingdom.
[h] Present address: Katedra Chemii Organicznej, Bioorganicznej i Biotechnologii, Krzywoustego 4, 44-100 Gliwice, Poland.
[i] Present address: Grupa Adamed, Pieńków 149, 05-152 Czosnów, Poland.

Glycolysis is an oxygen-independent ten-step enzymatic cascade converting one molecule of glucose into two molecules of pyruvate and yielding two molecules of ATP. Numerous cancer cell lines display a metabolic reprogramming (the so-called Warburg effect) characterized by an amplification of glucose uptake and glycolytic flux, even in the presence of oxygen, in order to provide for their heightened requirements in energy and building blocks for cell proliferation.[1–3] Associated with diverse oncogenic pathways such as c-MYC, HIF-1, PI3K/mTOR/AKT, RAS and BCR-ABL,[4,5] this adaptation constitutes a point of differentiation between cancerous and normal cells, and inhibition of glycolysis is therefore fitly considered as a promising approach for cancer treatment.[5,6] In this respect, the phosphofructokinase PFK-1, as first irreversible step of the glycolytic cascade (thus one of the key regulatory and rate limiting steps of glycolysis), constitutes a strategic point of intervention. PFK-1, in its tetrameric active form, catalyzes the conversion of fructose-6-phosphate (F-6-P) into fructose-1,6-bisphosphate (F-1,6-BP) and is regulated by over 20 allosteric effectors in various eukaryotes.[7] Among them, fructose-2,6-biphosphate (F-2,6-BP), produced from F-6-P by 6-phosphofructo-2-kinase/fructose-2,6-biphosphatases (PFKFBs), acts as its most potent activator.[8] Amidst the four known mammalian PFKFB isozymes, the ubiquitous and hypoxia induced form PFKFB3 has the highest kinase/phosphatase activity ratio (around 700),[9,10] and is overexpressed in many cancer types including colon, prostate, pancreatic, breast, thyroid, lung, ovarian, cancers and leukemia.[11,12] In this context, PFKFB3 plays a key role in maintaining high levels of F-2,6-BP thus promoting glycolysis through activation of PFK-1. As such, PFKFB3 has emerged as a potential target for cancer therapy.[12–14] One advantage over direct PFK1 blockade is that inhibition of PFKFB3 would not arrest the glycolytic flux, but maintain it at more basal levels.

This concept has been at the origin of several medicinal chemistry programs,[15–24] and in a previous study, we reported the discovery of potent PFKFB3 inhibitors based on a *N*-aryl 6-aminoquinoxaline scaffold.[25] Several compounds displayed two-digit nanomolar activity on target as well as single-digit micromolar inhibition of production of F-2,6-BP in HCT116 cells, such as compounds **1** and **2** (Fig. 1). The quinoxaline core anchors the scaffold in the ATP binding site of PFKFB3 through probable hydrogen bonds with ASN163 and SER152 as well as potential Pi-sulfur bonding with CYS154. Non-polar aromatic bicycles in position 8 of the quinoxaline penetrate a relatively flat lipophilic pocket and ortho-substituted amino aryl in position 6 tend to engage in Pi-stacking with TYR49 as well as Pi-anion interactions or hydrogen bonding with GLU166.

These compounds however suffer from low solubility and metabolic stability, and it was envisioned that the sulfone and carboxamide functions in **1** and **2** could serve as convenient handles to tackle these issues and fine-tune their physico-chemical properties *i.e.* by increasing their polarity. These functions being located at a relatively solvent-exposed area of the binding site (see figure 2, panel B), it was postulated that their modification would have a lesser impact on binding and activity.

Herein we report our efforts in that regard by the synthesis of novel series of amide and sulfonamide *N*-aryl 6-aminoquinoxaline derivatives based on **1** and **2**, their activity on PFKFB3 and improved physicochemical properties.

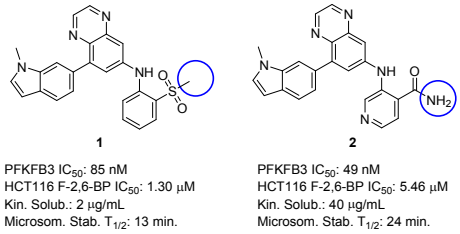

Figure 1. Compounds **1** and **2** *in vitro* activities, kinetic solubility (in Tris pH=8 buffer) and mouse liver microsomes stability (% remaining after 1 h incubation).

Scheme 1. Synthesis of representative compounds **5** and **7**.

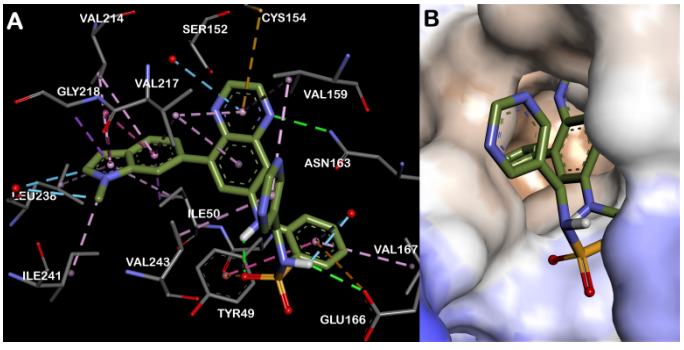

Figure 2. Crystal structure of compound **15** bound to the ATP pocket of PFKFB3 (PDB code: 6IBZ, resolution: 2.40 Å). A: interactions **15**-PFKFB3; B: highlighting the relative solvent exposure of the sulfonamide group.†

The synthesis of the compounds described herein was quite straightforward, using intermediates **3** and **6** whose preparation was described in a previous report.[25] Routes for representative examples **5** and **7** are shown in Scheme 1 (procedures and characterizations for all compounds and intermediates are given in Supporting Information). In the sulfonamide series, a 2-aniline moiety was chosen as linker between the sulfonamide and the quinoxaline core, the corresponding sulfones having demonstrated a higher F-2,6-BP production inhibition in human colorectal carcinoma cell line HCT116 than their pyrido counterparts. Inversely, the cellular activity was abolished in the case of compound **2**'s phenyl analogue, prompting us to keep a 3-aminopyridine moiety as linker for the carboxamide series.[25]

Both synthetic routes planned the diversity introduction as last step by parallel chemistry technics for efficiency, either by Buchwald-Hartwig coupling of 2-aminobenzenesulfonamides of type **5** with chloroquinoxaline **3**, or by peptide coupling with carboxylic acid **6**. Intermediates of type **5b** were obtained in two steps from 2-nitrobenzenesulfonyl chloride **3**, by Schotten-Baumann coupling with amines followed by nitro group reduction.

Generally, *N*-substituted sulfonamide derivatives showed an increase in activity on target compared to **8** (Table 1). This increase is most probably due to the emergence of additional Van der Waals interactions with residues in the corresponding zone of the binding site, such as VAL243, VAL159, VAL217, PRO421 and SER162. This zone appears mostly solvent exposed and London dispersive interactions with the substrate would minimize protein surface tension. A crystal structure of PFKFB3 in complex with compound **15** was solved and highlights such hydrophobic contacts (Figure 2, pink dotted lines). The "upward" orientation of the sulfonamide group appears stabilized by intramolecular hydrogen bonding between one of its oxygen atoms and the aromatic bridging NH, as well as by an hydrogen bond the sulfonamide NH and GLU166's carboxylate.

† Hydrophobicity surface represented. The orientation of the displayed hydrogen atoms was extrapolated to highlight the possible corresponding hydrogen bond interactions.

Table 1. Sulfonamide derivatives

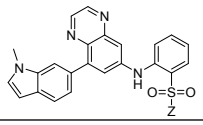

ID	Z	PFKFB3 IC_{50} [nM][a]	HCT116 F-2,6-BP IC_{50} [μM][b]	cLogD[c]	Kin. Solub. [μg/mL][d]	$T_{1/2}$ [min.][e]	ID	Z	PFKFB3 IC_{50} [nM][a]	HCT116 F-2,6-BP IC_{50} [μM][b]	cLogD[c]	Kin. Solub. [μg/mL][d]	$T_{1/2}$ [min.][e]
8	NH_2	265	37.61	3.3	6	30	**14**		33	3.16	3.3	26	40
9	NHMe	104	>100	3.5	2	12	**15**		22	>100	3.3	3	6
10	NMe_2	94	7.67	3.8	2	14	**16**		62	>100	3.6	3	12
11		1692	>100	2.6	254	41	**17**		38	>100	3.7	2	16
12		36	2.64	3.5	5	22	**18**		26	>100	4.0	2	18
13		59	9.78	3.8	9	29	**5**		11	4.64	2.8	35	38

[a] Determined by biochemical PFKFB3 activity inhibition assay (ADP-Glo™);
[b] Data reported are the mean of at least n = 2 independent experiments with SEM ± 0.2 log units
[c] $LogD_{7.4}$ values were predicted by Instant JChem[26]
[d] Measured in Tris buffer at pH 8
[e] Half life, mouse liver microsomal stability

Among the sulfonamide derivatives tested, compounds bearing ionizable groups at physiological pH (7.4), were expected to display increased kinetic solubilities and metabolic stabilities, as is the case for **11** and **5**. Compound **11**, featuring an acidic sulfonamide (pKa ≈ 6.5, 88% of microspecies in anionic state at pH = 7.4),[27] however lost activity, probably due to the repulsion of this delocalized negative charge by GLU166 as well as permeability reduction/efflux. On the other hand, compound **5** is likely to be encountered in its *N*-methyl pyrrolidinium form (pKa ≈ 8.2 for **5**, 86% of cationic microspecies at pH = 7.4). On top of exhibiting slightly improved solubility and metabolic stability, **5** displayed the best activities on target for the sulfonamide series (11 nM) and maintained reasonable cellular activity (4.64 μM). Docking studies on this compound suggested the formation of a salt bridge between the ammonium group and GLU166, accounting for the good activity of **5**.

Other cyclic aliphatic amines such as **13** and **14**, for which pKa was predicted around 7.2, dwell mainly in their neutral state at physiological pH, only offered a slight advantage in term of activity. However, with around 39% of microspecies predicted to be in ammonium form, these compounds showed moderate to good metabolic stability. The same outcome was not observed with weaker heteroaromatic bases (**15**-**17**), displaying low $T_{1/2}$ and loss of cellular activity in spite of acceptable potency on target. Methylation of the sulfonamide nitrogen, in the hope to increase permeability and cellular activity, was accompanied by reduction of activity on PFKFB3, presumably due to the suppression of a potential hydrogen bond with GLU166.

Results in the carboxamide series were more gratifying (Table 2). Apart from planar compounds **19**, **21** and **23**, all amides synthesized displayed satisfying kinetic solubilities. Di-substitution on the amide nitrogen (compounds **20** and **38**) proved detrimental for activity, showing the importance of the potential hydrogen bond with GLU166 for binding in this series (see Fig. 3 and Fig. 4). In the case of heteroaromatic derivatives (pyrimidines and pyrazoles **21**-**24**), in contrast with the sulfonamide series, solubilities were greatly improved when the aromatic was connected to the amide through a methylene linker (compounds **22** and **24**). This was unfortunately accompanied by a five-fold reduction in activity on target in comparison to their directly linked counterparts **21** (22 nM) and **23** (33 nM), possibly due to the entropy-increasing addition of an extra rotatable bond and a possible steric clash with PRO421. Contrarily to its anionic sulfonamide analog **11**, pyrimidine **21** remains neutral at pH 7.4 (pKa ≈ 12.4), allowing for binding with PFKFB3 (on-target IC_{50}: 22 nM) cellular target engagement (HCT116 IC_{50}: 3.5 μM). Generally, heteroaromatic derivatives showed high intrinsic clearance in mouse microsomal stability and were dismissed.

A crystal structure of compound **21** bound to the ATP pocket of PFKFB3 was solved and highlights key interactions accounting for the common conformational features observed throughout the carboxamide series (Figure 3). The $C{=}O_{carboxamide}$ group is oriented towards the NH linked to the quinoxaline core with which it interacts by intramolecular hydrogen bonding, whereas the $NH_{carboxamide}$ engages in hydrogen bonding with the carboxylate of GLU166.

Table 2. Carboxamide derivatives

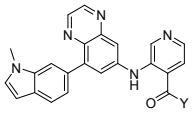

ID	Y	PFKFB3 IC_{50} [nM][a]	HCT116 F-2,6-BP IC_{50} [μM][b]	cLogD[c]	Kin. Solub. [μg/mL][d]	$T_{1/2}$ [min.][e]	ID	Y	PFKFB3 IC_{50} [nM][a]	HCT116 F-2,6-BP IC_{50} [μM][b]	cLogD[c]	Kin. Solub. [μg/mL][d]	$T_{1/2}$ [min.][e]
19	NHMe	83	7.02	3.9	4	27	**30**		11	13.49	3.6	212	24
20	NMe_2	499	>100	4.1	175	21	**31**		116	96.52	3.4	253	45
21		22	3.50	4.0	4	25	**32**		33	41.74	2.8	239	> 60
22		106	49.47	3.7	233	24	**33**	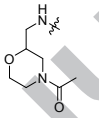	93	>100	2.9	268	13
23		33	26.50	4.3	2	12	**34**		30	9.19	3.7	170	> 60
24		159	75.92	4.0	127	16	**35**		73	97.38	3.0	244	49
25		38	19.46	2.7	246	> 60	**36**	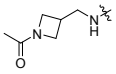	137	>100	3.0	252	> 60
26	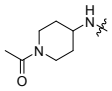	18	31.26	3.1	213	7	**7**		15	8.28	3.2	229	51
27		69	56.45	2.9	242	> 60	**37**		74	24.01	2.3	246	> 60
28		41	48.77	3.2	48	43	**38**		176	39.69	3.3	245	> 60
29		2	8.37	3.8	246	51	**39**		105	>100	3.1	253	40

[a] Determined by biochemical PFKFB3 activity inhibition assay (ADP-Glo™)
[b] Data reported are the mean of at least n = 2 independent experiments with SEM ± 0.2 log units
[c] $LogD_{7.4}$ values were predicted by Instant JChem[26]
[d] Measured in Tris buffer at pH 8
[e] Half life, mouse liver microsomal stability

Hydrophobic contacts are observed between the amide substituent and VAL243 as well as PRO421. In the case of compound **21**, the observed orientation of the pyrimidine group is stabilized by weak non-conventional hydrogen bonds with COO_{GLU166} and OH_{TYR49}, as well as hydrogen bonding of one of its nitrogen atoms with a very well conserved water molecule linked to GLN243. The crystal structure of compound **23** in complex with PFKFB3 (data not shown) revealed that although the pyrazole ring adopted a very similar conformation, it did not interact with this conserved water molecule, probably explaining the slight activity difference between **21** and **23**.

We then turned our attention towards aliphatic heterocycles (compounds **25**-**39**), which proved to be more promising.

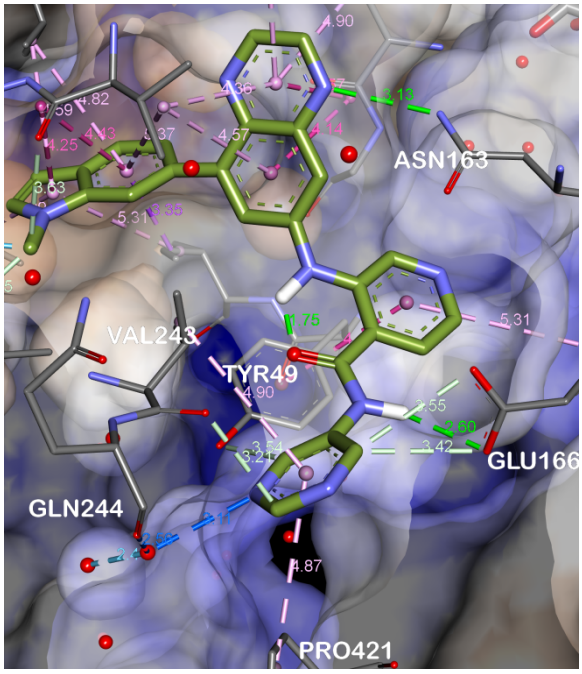

Figure 3. Crystal structure of compound **21** bound to the ATP pocket of PFKFB3 (PDB code: 6ICO, resolution: 2.60 Å).‡

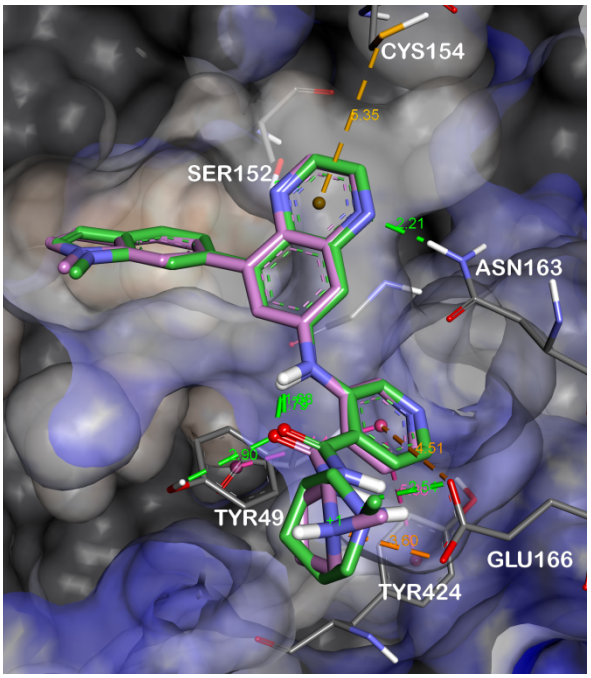

Figure 4. Superimposed crystal structures of compounds **29** (in green, PDB code: 6IBX, resolution: 2.11 Å) and **7** (in pink, PDB code: 6IBY, resolution: 2.51 Å protein not shown).‡

Apart from 6-member cyclic acetamide derivatives **26**, **30**, and **33**, probably subject to de-acetylation, metabolic stability was generally good in this series. De-acetylation was less pronounced for compounds **35**, **36** and **39**. In the case of **35** and **36**, it correlates with the fact that azetidines are generally more metabolically stable than the corresponding 5- and 6-member rings due to their lower intrinsic LogP.[28] Generally, the presence of an extra carbonyl function, either as acetamide group, or on the cycle itself (compounds **27** and **31**) was favorable for solubility, providing further opportunities for hydrogen bonding with the solvent.

Additionally, given the smaller inductive electron-withdrawing effect of carboxamides compared to sulfonamides, most basic aliphatic heterocyclic compounds prepared are predicted to remain in their polar ammonium form at physiological pH, proving beneficial for their solubility and metabolic stability.

Crystal structures of PFKFB3 in complex with ammonium compounds **25** (not shown), **29** and **7** have been solved and confirmed the formation of a postulated salt bridge with GLU166 (see Figure 4). Compounds **29** and **7** showed the best activity on target with IC_{50}s of 2 nM and 15 nM respectively, in accordance with the measured distances between the ammonium groups and the carboxylate function (2.23 Å for **29** and 3.75 Å for **7**). The 4-position of the ammonium group in **25** is less favorable for its interaction with GLU166 (d = 4.69 Å) seemingly resulting in a lower activity than **29**. In the case of both **29** and **7**, X-ray structures displayed *R* configuration enantiomer in complex with PFKFB3.

As a consequence of their neutral form, most acetamide and cyclic amide derivatives proved less active than their amine counterparts. This was corroborated by cellular activities with IC_{50}s higher than 30 µM. Compound **30** still conserved an average cellular activity (IC_{50} = 13.5 µM), with an activity on target at 11 nM, the best scoring docking pose of its *R* enantiomer suggesting the possibility of a strong hydrogen bond between $C{=}O_{acetamide}$ and $NH_{2\ GLN243}$.

With these results in hand, considering the poor solubilities and moderate to low metabolic stabilities of the sulfonamide compounds, we decided to focus our efforts in the carboxamide series, more particularly using 3-amino-1-methylpyrrolidin-1-ium derivatives, compound **7** displaying a slightly better cellular activity than **29**. In a previous study,[25] we identified several indole replacements which proved beneficial for activity and/or physicochemical properties. For instance, a 1,3-benzothiazol-2-amine moiety reduced LogD and improved solubility and metabolic stability while maintaining a good activity on target. On the other hand, 3-methyl-benzothiophene and 4-fluoro-1-methylindole slightly increased LogD and improved cellular and on-target activities. The corresponding derivatives were synthesized (see Supporting information) and the results are shown in Table 3.

Thiophene derivatives **40** and **41**, with a higher LogD, demonstrated improved cellular activities ($IC_{50} \approx 3$ µM). As hinted by X-Ray crystallography, the *R* enantiomer appeared slightly more active on target than the *S,* however, the marginal difference (IC_{50}s of 4 nM and 9 nM respectively) did not justify pursuing with enantiomerically pure compounds. On the other hand, compounds **40** and **41** suffered from lower solubilities and slightly higher mouse microsomes clearances than indole derivative **7**. 1,3-Benzothiazol-2-amine compound **42** showed remarkable metabolic stability and solubility ($T_{1/2}$ > 60 min. Kin_{solub} = 241 µg/mL), however at the expense of a reduced cellular activity (IC_{50} ≈ 7 µM), probably due to a diminution of cell membrane permeability concomitant with an increase of the hydrogen bond donor count. Adding a fluorine atom in position 4 of the indole moiety (compound **43**) increased metabolic stability compared to **7** while maintaining good kinetic solubility (185 µg/mL). Although equipotent with **7** on target, **43** displayed a 20-fold improvement of cellular activity at 0.48 nM, qualifying it as the best compound of our study.

‡ Hydrophobicity surface represented. The orientation of the displayed hydrogen atoms was extrapolated to highlight the possible corresponding hydrogen bond interactions.

Table 3. Carboxamide derivatives

ID	Y	PFKFB3 IC_{50} [nM][a]	HCT116 F-2,6-BP IC_{50} [μM][b]	cLogD[c]	Kin. Solub. [μg/mL][d]	$T_{1/2}$ [min.][e]
40	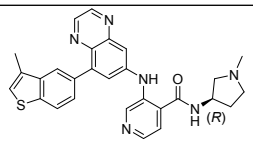	4	2.72	4.9	79	36
41	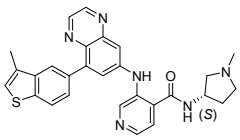	9	3.34	4.9	80	48
42	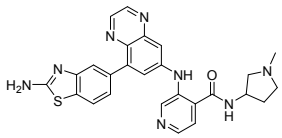	35	6.95	2.9	241	> 60
43	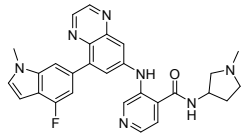	17	0.48	3.9	185	> 60

[a] Determined by biochemical PFKFB3 activity inhibition assay (ADP-Glo™)
[b] Data reported are the mean of at least n = 2 independent experiments with SEM ± 0.2 log units
[c] $LogD_{7.4}$ values were predicted by Instant JChem[26]
[d] Measured in Tris buffer at pH 8
[e] Half life, mouse microsomal stability

In conclusion, we synthetized a novel series of *N*-aryl 6-aminoquinoxalines as PFKFB3 inhibitors with improved physicochemical properties. The carboxamide series (compounds **19-43**) displayed increased kinetic solubility and metabolic stability compared to its sulfonamide counterpart. The best activities were observed with (3*R*)-3-carboxamido-1-methylpyrrolidin-1-ium derivatives able to form a salt bridge with PFKFB3's GLU166 residue. Their ionic ammonium form at physiological pH did not hamper their cellular activity, with compound **43** displaying IC_{50}s of 17 nM on target and of 480 nM for the inhibition of F-2,6-BP production in HCT116 cells. Compound **43** shows excellent solubility and mouse microsomes metabolic stability and the series is currently the object of *in-vivo* evaluations. These compounds may provide useful tools to better understand the role of the PFKFB3 in cancer metabolism.

Acknowledgments

This work was supported by the European Regional Development Fund under The Operational Program Innovative Economy, 2007-2013, measure 1.4 (POIG.01.04.00-12-120/12-00). The authors would like to thank Maja Potocki, and Małgorzata Cebo for their assistance in compound purification. We are grateful to Marek Żylewski for 400 MHz NMR, to Marta Flinta and Liliana Luchowska for LCMS analyses, and to Ewelina Gabor-Worwa, Agnieszka Przybyłowicz, Bożena Winnik and Agata Dudek for ADME characterizations.

References and notes

1. Warburg O. On the Origin of Cancer Cells. *Science*. 1956;123(3191):309-314. doi:10.1126/science.123.3191.309.
2. Weinhouse S. On Respiratory Impairment in Cancer Cells. *Science*. 1956;124(3215):267-272. doi:10.1126/science.124.3215.267.
3. Vander Heiden MG, Cantley LC, Thompson CB. Understanding the warburg effect: The metabolic requirements of cell proliferation. *Science*. 2009;324(5930):1029-1033. doi:10.1126/science.1160809.
4. Tarrado-Castellarnau M, de Atauri P, Cascante M. Oncogenic regulation of tumor metabolic reprogramming. *Oncotarget*. 2016;7(38):62726-62753. doi:10.18632/oncotarget.10911.
5. Pelicano H, Martin DS, Xu RH, Huang P. Glycolysis inhibition for anticancer treatment. *Oncogene*. 2006;25(34):4633-4646. doi:10.1038/sj.onc.1209597.
6. Counihan JL, Grossman EA, Nomura DK. Cancer Metabolism: Current Understanding and Therapies. *Chem Rev*. 2018;118(14):6893-6923. doi:10.1021/acs.chemrev.7b00775.
7. Schöneberg T, Kloos M, Brüser A, Kirchberger J, Sträter N. Structure and allosteric regulation of eukaryotic 6-phosphofructokinases. *Biol Chem*. 2013;394(8):977-993. doi:10.1515/hsz-2013-0130.
8. Van Schaftingen E, Hue L, Hers HG. Fructose 2,6-bisphosphate, the probably structure of the glucose- and glucagon-sensitive stimulator of phosphofructokinase. *Biochem J*. 1980;192(3):897-901. doi:10.1042/bj1920897.
9. Manzano A, Rosa JL, Ventura F, et al. Molecular cloning, expression, and chromosomal localization of a ubiquitously expressed human 6-phosphofructo-2-kinase/ fructose-2, 6-bisphosphatase gene (PFKFB3). *Cytogenet Cell Genet*. 1998;83(3-4):214-217. doi:15181.
10. Sakakibara R, Kato M, Okamura N, et al. Characterization of a Human Placental Fructose-6-Phosphate, 2-Kinase/Fructose- 2,6 - Bisphosphatase. *J Biochem*. 1997;122(1):122-128. doi:10.1093/oxfordjournals.jbchem.a021719.
11. Atsumi T, Chesney J, Metz C, et al. High expression of inducible 6-phosphofructo-2-kinase/fructose-2,6-bisphosphatase (iPFK-2; PFKFB3) in human cancers. *Cancer Res*. 2002;62(20):5881-5887. http://www.ncbi.nlm.nih.gov/pubmed/12384552.
12. Shi L, Pan H, Liu Z, Xie J, Han W. Roles of PFKFB3 in cancer. *Signal Transduct Target Ther*. 2017;2(April):17044. doi:10.1038/sigtrans.2017.44.

13. Chesney J. 6-Phosphofructo-2-kinase/fructose-2,6-bisphosphatase and tumor cell glycolysis. *Curr Opin Clin Nutr Metab Care*. 2006;9(5):535-539. doi:10.1097/01.mco.0000241661.15514.fb.
14. Lu L, Chen Y, Zhu Y. The molecular basis of targeting PFKFB3 as a therapeutic strategy against cancer. *Oncotarget*. 2017;8(37):62793-62802. doi:10.18632/oncotarget.19513.
15. Seo M, Kim J-D, Neau D, Sehgal I, Lee Y-H. Structure-Based Development of Small Molecule PFKFB3 Inhibitors: A Framework for Potential Cancer Therapeutic Agents Targeting the Warburg Effect. *PLoS One*. 2011;6(9):e24179. doi:10.1371/journal.pone.0024179.
16. Boyd S, Brookfield JL, Critchlow SE, et al. Structure-based design of potent and selective inhibitors of the metabolic kinase PFKFB3. *J Med Chem*. 2015;58(8):3611-3625. doi:10.1021/acs.jmedchem.5b00352.
17. St-Gallay SA, Bennett N, Critchlow SE, et al. A High-Throughput Screening Triage Workflow to Authenticate a Novel Series of PFKFB3 Inhibitors. *SLAS Discov*. 2018;23(1):11-22. doi:10.1177/2472555217732289.
18. Telang S, Chesney J, Trent JO. Selective PFKFB4 inhibitors for the treatment of cancer. *PCT Int Appl*. 2016;(WO2016172499):130pp.
19. Clem B, Telang S, Clem A, et al. Small-molecule inhibition of 6-phosphofructo-2-kinase activity suppresses glycolytic flux and tumor growth. *Mol Cancer Ther*. 2008;7(1):110-120. doi:10.1158/1535-7163.MCT-07-0482.
20. Chand P, Chesney JA, Clem BF, Tapolsky GH, Telang S, Trent JO. Small molecule inhibitors of 6-phosphofructo-2-kinase/fructose-2,6-biphosphate 3 and glycolytic flux and their methods of use as anti-cancer therapeutics. *PCT Int Appl*. 2011;(WO2011103557):65pp.
21. Angbrant J, Homan E, Lundbaeck T, et al. Preparation of Bisarylsulfonamides as Inhibitors of 6-phosphofructo-2-kinase/fructose-2,6-bisphosphatase PFKFB3 and PFKFB4 Isoforms Useful in the Treatment of Inflammation and Cancer. *PCT Int Appl*. 2011;(WO2011161201):213pp.
22. Bystroem S, Hedgecock C, Homan E, et al. Preparation of (hetero)aryl sulfonamides for treating inflammation and cancer. *PCT Int Appl*. 2012;(WO2012035171):149pp.
23. Telang S, O'Neal J, Tapolsky G, et al. Discovery of a PFKFB3 inhibitor for phase I trial testing that synergizes with the B-Raf inhibitor vemurafenib. *Cancer Metab*. 2014;2(Suppl 1):P14. doi:10.1186/2049-3002-2-S1-P14.
24. Tsuhako AL, Marlowe CK, Zaharia CA, et al. Pyrimidine derivatives as inhibitors of inducible form of 6-phosphofructose-2-kinase and their preparation and use for the treatment of cancer. *PCT Int Appl*. 2012;(WO2012149528A1):418pp.
25. Boutard N, Białas A, Sabiniarz A, et al. Discovery and Structure-Activity Relationships of N-Aryl 6-Aminoquinoxalines as Potent PFKFB3 Kinase Inhibitors. *ChemMedChem*. 2018;in press. doi:10.1002/cmdc.201800569.
26. Instant JChem v17.2 2017 (ChemAxon, Budapest, Hungary). 2017. http://www.chemaxon.com.
27. MarvinSketch 16.2.22.0 pKa plugin (ChemAxon, Budapest, Hungary). 2016. http://www.chemaxon.com.
28. St. Jean DJ, Fotsch C. Mitigating Heterocycle Metabolism in Drug Discovery. *J Med Chem*. 2012;55(13):6002-6020. doi:10.1021/jm300343m.

Supplementary Material

Supplementary data associated with this article can be found, in the online version, at

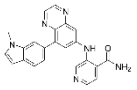

2

PFKFB3 IC_{50}: 49 nM
HCT116 F-2,6-BP IC_{50}: 5.46 µM
Kin. Solub.: 40 µg/mL
Microsom. Stab. $T_{1/2}$: 24' min.

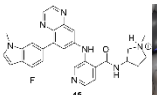

45

PFKFB3 IC_{50}: 17 nM
HCT116 F-2,6-BP IC_{50}: 0.48 uM
Kin. Solub.:185 µg/mL
Microsom. Stab. $T_{1/2}$: > 60 min.

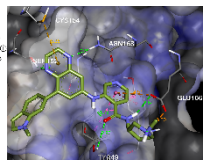

Author contributions and ORCID identifiers:

	Co-author	Email and affiliation if not Selvita	Contribution	ORCID identifier
1	Nicolas Boutard	nicolas.boutard@selvita.com Selvita SA Medicinal Chemist Selvita SA Discovery Chemistry Ul. Bobrzyńskiego 14 Kraków 30-348	Writing Original Draft: Lead Investigation: Equal Supervision: Equal Formal analysis: Equal Software: Lead Visualization: Lead	0000-0002-0976-5080
2	Arkadiusz Białas	arkadiusz.bialas@selvita.com	Investigation: Equal Supervision: Equal Writing Review And Editing: Supporting	
3	Aleksandra Sabiniarz	aleksandra.sabiniarz@selvita.com	Investigation: Equal Supervision: Equal	0000-0001-5888-9728
4	Paweł Guzik	pawel.guzik@selvita.com	Investigation: Equal Supervision: Equal Writing review and editing: Supporting	0000-0003-3939-5778
5	Katarzyna Banaszak	katarzyna.banaszak@selvita.com	Investigation: Equal Formal analysis: Equal Data curation: Equal Software: Lead Writing review and editing: Supporting	0000-0001-7096-679X
6	Artur Biela	biela.artur@gmail.com	Investigation: Supporting	
7	Marcin Bień	marcin.d.bien@gmail.com	Investigation: Supporting	
8	Anna Buda	anna.buda@selvita.com	Investigation: Supporting	0000-0001-9365-6153
	Barbara Bugaj	barbara.bugaj@selvita.com	Investigation: Supporting	
9	Ewelina Cieluch	ewelina.cieluch@selvita.com	Investigation: Supporting	
10	Anna Cierpich	anna.cierpich@gmail.com	Investigation: Supporting	
11	Łukasz Dudek	lukasz.dudek@selvita.com	Investigation: Supporting	
12	Hans-Michael Eggenweiler	Hans-Michael.Eggenweiler@merckgroup.com	Conceptualization: Lead Funding acquisition: Lead Project Administration: Lead Supervision: Lead Formal Analysis: Lead	0000-0003-2202-5826
13	Joanna Fogt	joanna.fogt@selvita.com	Investigation: Supporting	0000-0002-9296-2164
	Monika Gaik	monika.gaik@uj.edu.pl	Investigation: Supporting	0000-0003-4939-3821

	Co-author	Email and affiliation if not Selvita	Contribution	ORCID identifier
14	Andrzej Gondela	andrzej.gondela@selvita.com	Investigation: Supporting	
15	Krzysztof Jakubiec	krzysztof.jakubiec@selvita.com	Investigation: Supporting Writing Review And Editing: Equal	
16	Mirek Jurzak	Mirek.Jurzak@merckgroup.com	Conceptualization: Lead Funding acquisition: Lead Project Administration: Lead Supervision: Lead Formal Analysis: Lead	
17	Agata Kitlińska	agata.kitlinska@selvita.com	Investigation: Supporting	
18	Piotr Kowalczyk	piotr.kowalczyk@selvita.com	Funding acquisition: Lead	0000-0001-9499-2095
19	Maciej Kujawa	maciej.kujawa@selvita.com	Investigation: Supporting	0000-0002-8659-7404
20	Katarzyna Kwiecińska	kwiecinskaxyz@gmail.com	Investigation: Supporting	0000-0001-6803-6585
21	Marcin Leś	marcin.les@selvita.com	Investigation: Supporting	
22	Ralph Lindemann	ralph.lindemann@merckgroup.com	Conceptualization: Lead Funding acquisition: Lead Project Administration: Lead Supervision: Lead Formal Analysis: Lead	0000-0003-2399-3992
23	Monika Maciuszek	maciuszekmonika@gmail.com	Investigation: Supporting Writing Review And Editing: Equal	0000-0003-1182-1544
24	Maciej Mikulski	maciej.mikulski@selvita.com	Investigation: Supporting	0000-0002-3233-115X
25	Paulina Niedziejko	paulina.niedziejko@selvita.com	Investigation: Supporting	0000-0003-0520-112X
26	Alicja Obara	alicja.obara@selvita.com	Investigation: Supporting	
27	Henryk Pawlik	henrykpawlik@gmail.com	Investigation: Supporting	
28	Tomasz Rzymski	tomasz.rzymski@selvita.com	Funding acquisition: Lead	
29	Magdalena Sieprawska-Lupa	magdalena.sieprawska@selvita.com	Supervision: Equal Supervision: Supporting	
30	Marta Sowińska	marta.sowinska@selvita.com	Investigation: Supporting	
31	Joanna Szeremeta-Spisak	joanna.spisak@selvita.com	Investigation: Supporting	0000-0002-4572-784X
32	Agata Stachowicz	agata.stachowicz@selvita.com	Investigation: Supporting	

	Co-author	Email and affiliation if not Selvita	Contribution	ORCID identifier
33	Mateusz M. Tomczyk	Mateusz.Tomczyk@polsl.pl	Investigation: Supporting	0000-0002-9594-4535
34	Katarzyna Wiklik	katarzyna.wiklik@selvita.com	Investigation: Equal Formal analysis: Equal Software: Lead Visualization: Lead Writing review and editing: Supporting	0000-0001-6364-7088
35	Łukasz Włoszczak	lukewloszcz@gmail.com	Investigation: Supporting	0000-0001-5093-1397
	Sylwia Ziemiańska	sylwia.buczek@selvita.com	Investigation: Supporting	
36	Adrian Zarębski	adrian.zarebski@selvita.com	Investigation: Equal Validation: Lead Supervision: Equal Data curation: Lead Writing review and editing: Supporting	
37	Krzysztof Brzózka	krzysztof.brzozka@selvita.com	Conceptualization: Lead Funding acquisition: Lead Project Administration: Lead Supervision: Lead Formal Analysis: Lead	
38	Mateusz Nowak	mateusz.nowak@selvita.com	Conceptualization: Lead Funding acquisition: Lead Project Administration: Lead Supervision: Lead Formal Analysis: Lead	0000-0002-5261-0375
39	Charles-Henry Fabritius	charles.fabritius@selvita.com	Supervision: Lead Investigation: Lead Data curation: Lead Formal analysis: Lead Software: Equal Visualization: Equal Writing review and editing: Lead	